PERIODICA POLYTECHNICA SER. TRANSP. ENG. VOL. 30, NO. 1–2, PP. 69–92 (2002)

NONLINEAR MODELLING AND MODEL VERIFICATION OF A SINGLE PROTECTION VALVE

Huba NÉMETH*, Piroska AILER** and Katalin M. HANGOS***

*Knorr-Bremse Research & Development Centre
H–1119, Budapest, Major u. 69., Hungary
**Aviation Technical Institute
Miklós Zrínyi National Defense University
H–5008, Szolnok, P.O.B. 1., Hungary
***Systems and Control Laboratory
Computer and Automation Research Institute
Hungarian Academy of Sciences
H–1518, Budapest, P.O.B. 63., Hungary

Received: Sept. 24 2002, Revised: Dec. 12, 2002

Abstract

A lumped parameter dynamic model of a single protection valve with electronic actuation in a brake system based on first engineering principles is presented in this paper for control design purposes. The model is developed in an index-1 differential-algebraic equation (DAE) form, and it is capable of describing the hybrid behaviour of the protection valve. The DAE model is transformed into its standard nonlinear input-affine state-space model form, which will be used for control design purposes.

The developed model has been verified by simulation studies, where it is shown that it is capable to describe the dynamic behavior of the examined protection valve.

Keywords: brake system, nonlinear, hybrid model, fluid- and thermodynamics, mechanics, electromagnetics.

1. Introduction

The application of protection valves in conventional air brake systems has nowadays become common and new generation air supply systems with integrated electronic control will use this onward with slight modifications. Thus the dynamic behavior and properties of protection valves have become essential for designing such a system [2]. Therefore the main aim of this paper is to develop and verify a lumped parameter dynamic model of protection valves for control design purposes based on first engineering principles.

From the viewpoint of air conservation, commercial vehicle air brake systems can be divided into three main hierarchical parts (see *Fig. 1*): the air supply, air treatment and air consumption subsystems. The air supply part has only one operating unit: the compressor (denoted by 3 in the Figure). The air consumption part has several units carrying out the control of the brake chamber pressure to satisfy the

driver's deceleration demand. Furthermore, air spring and some auxiliary systems (e.g. boosters) belong to the air consumption subsystem, too.

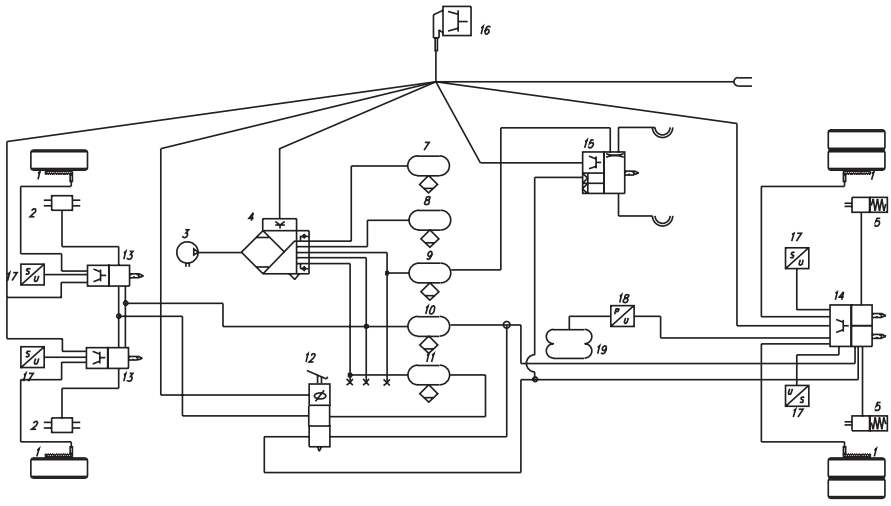

Fig. 1. Layout of electropneumatic brake system with electronic air treatment of a towing vehicle (4x2)

Air treatment and control systems (denoted by 4 in the Figure), being in the focus of this paper, consist of three main functional parts: the system pressure controller, the air-drying and air distribution units in the brake circuits. This last component consists of protection valves, which ensure the independence and safety of circuits, as well as they set up the circuit fill up sequence. The number of these valve elements is the same as the number of independent circuits (typically four or five).

In present and future air treatment systems protection valves are equipped with electronic pressure limiting in order to avoid pneumatic limiter and thereby reduce cost. To develop the proper controller, it is required to develop a dynamic system model of the protection valve [3, 4]. Considering that the pressure limiting is controlled at a sampling frequency in the order of magnitude of 100 Hz [8], dynamic behavior of the pneumatic components must also be taken into account in the design of electronic air supply system composition and control, if appropriate circuit fill operation is to be guaranteed, especially when no reservoir is present in the corresponding circuit [7].

2. Nonlinear Model of a Single Protection Valve

The lumped nonlinear state-space model of the single protection valve is developed in several steps following a standard general modelling procedure for process systems [5].

2.1. System Description

The single circuit protection valve with its close surrounding to be modelled consists of the following elements (see *Fig. 2*):

- **Input chamber** (1) This chamber has an input air flow from the compressor and two output flows towards the protection valve and the magnet valve.
- **Output chamber** (2) This chamber has an input air flow from the protection valve and an output towards the brake system or other consumers.
- **Control chamber** (3) This chamber has a single connection that can be connected either to the input chamber or the environment by the magnet valve.
- **Input piping** (4) It connects the input chamber to the protection valve.
- **Output piping** (5) This is the connection between the protection valve and the outlet chamber.
- **Protection valve** (6) The valve has an input connection from the input chamber through the input pipe and an output to the output chamber through the output pipe.
- **Control magnet valve** (7) It is a 3/2-way valve with solenoid excitation with one input connected to the input chamber and two outputs. The one is going to the control chamber and the other one is exhausting to the environment.

The input chamber represents the compressor piping volume and coupled circuits with opened protection valve, while the output chamber serves as the effective reservoir of the circuit.

2.2. Modelling Goal and Accuracy Requirements

The aim of the modelling is to use the developed model for dynamic simulation, system identification and process control. Therefore the resulted model should describe the dynamic behavior of the real process only within 10% desired accuracy [5].

2.3. Control Aims

The following control aims are considered for circuit pressure limiting features of the electromagnetic protection valve:

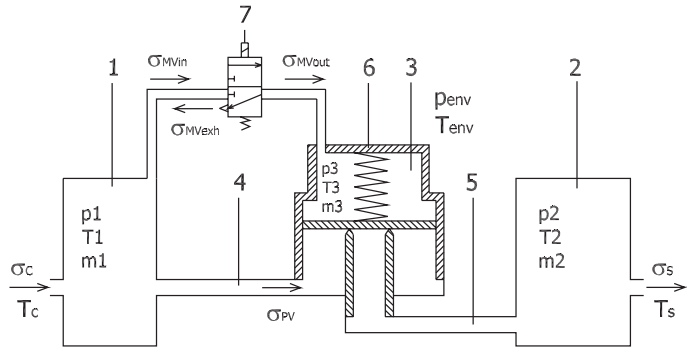

Fig. 2. Schematic diagram of single electromagnetic protection valve

$\mathcal{C}1$. The circuit pressure has to be limited according to a target pressure with 500 mbar tolerance.

$\mathcal{C}2$. The control has to be robust with respect to the external disturbances and the parameters of the linearised model.

2.4. Modelling Assumptions

When constructing the model of the considered single protection valve system shown in *Fig.2*, the following assumptions have been made in order to reduce complexity:

$\mathcal{A}1$. The gas physical properties such as specific heats, gas constant and adiabatic exponent are assumed to be constant over the whole time, pressure and temperature domain.

$\mathcal{A}2$. All chamber pressures are higher or equal to the environment pressure.

$\mathcal{A}3$. The gas in the chambers is perfectly mixed, no spatial variation is considered.

$\mathcal{A}4$. The magnet valve elements are modelled assuming linear magneto-dynamically homogeneous material.

$\mathcal{A}5$. Heat radiation is neglected.

$\mathcal{A}6$. Compressor airflow is assumed to have non-negative values only, all other airflows can have negative and positive values as well depending on the flow direction.

$\mathcal{A}7$. The magnet valve body maximal stroke, inlet and exhaust port diameters are assumed to satisfy the inequality: $x_{MV\,\max} > \frac{d_{MVin}}{4} + \frac{d_{MVexh}}{4}$.

$\mathcal{A}8$. The magnet valve port cross sections are assumed to satisfy the condition: $A_{MVout} >> A_{MVin}, A_{MVexh}$.

2.5. Hybrid Behavior

The system contains several parts that exhibit non-continuous or non-smooth behavior. This means that the equations which describe the dynamic behavior of the corresponding subsystem vary according to certain circumstances as discussed in [5].

An example for this property is shown on the limiting force equation of the protection valve piston. In this case three hybrid states with different model equations are applied to the same term $F_{PV\,\mathrm{lim}}$ depending on the piston stroke:

Protection valve limiting force Hybrid-State 1: When the protection valve is closed ($x_{PV} < 0$), the stroke limiting force is given by:

$$F_{PV\,\mathrm{lim}} = -c_{PV\,\mathrm{lim}} x_{PV}. \tag{1}$$

Protection valve limiting force Hybrid-State 2: When the valve is in intermediate opening position ($0 \leq x_{PV} \leq x_{PV\,\mathrm{max}}$), there is a zero force to limit the stroke as:

$$F_{PV\,\mathrm{lim}} = 0. \tag{2}$$

Protection valve limiting force Hybrid-State 3: When reaching maximal opening stroke ($x_{PV} > x_{PV\,\mathrm{max}}$), the limiting force of the protection valve is computed as:

$$F_{PV\,\mathrm{lim}} = -c_{PV\,\mathrm{lim}} \left(x_{PV} - x_{PV\,\mathrm{max}}\right). \tag{3}$$

The state transition graph of the above hybrid states can be seen in *Fig.3*.

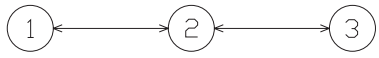

Fig. 3. State transition graph of protection valve stroke limiting force

2.5.1. Hybrid Items of the Model

The developed model includes four parts that have hybrid behavior. These parts are arranged according to the included hybrid state-dependent terms as follows:

- Gas energy equations
  - Input chamber (4 hybrid states)
  - Output chamber (4 hybrid states)
  - Control chamber (2 hybrid states)
- Streaming cross-section equations
  - Protection valve (2 hybrid states)

  - Magnet valve (5 hybrid states)
- Stroke limiting force equations
  - Protection valve (3 hybrid states)
  - Magnet valve (3 hybrid states)
- Air flows and gas speed equations
  - Protection valve (5 hybrid states)
  - Magnet valve (4+2 hybrid states)

The total number of hybrid states is then 34. The complete model with all hybrid states included can be found in [1].

From now only one hybrid state is discussed with each of the above hybrid behavior items having a specific well-defined state. This means that a special dedicated hybrid state is selected for each hybrid item.

This investigated special hybrid state corresponds to *the fill up procedure of output chamber (brake circuit)*. In this state the input chamber is filled by the compressor meanwhile the output chamber has lower pressure producing a positive direction air flow through the protection valve, where the protection valve stroke has an intermediate position (no stroke limiting). The streaming process is subsonic. The magnet valve is not excited so no air flow is considered through that.

2.6. Conservation Equations

The balance equations are developed from conservation principles for mass and energy. The notation list can be found in the Appendix.

2.6.1. Gas Mass Balance

In order to describe the gas mass balances in the system three balance volumes are defined that include the whole volume of all the three chambers (see *Fig.2*).

The balance of gas mass in the chambers can be written as:

$$\frac{\mathrm{d}m_1}{\mathrm{d}t} = \sigma_C - \sigma_{PV} - \sigma_{MVin}, \tag{4}$$

$$\frac{\mathrm{d}m_2}{\mathrm{d}t} = \sigma_{PV} - \sigma_S, \tag{5}$$

$$\frac{\mathrm{d}m_3}{\mathrm{d}t} = \sigma_{MVout}. \tag{6}$$

2.6.2. Gas Internal Energy Balance

Using the same balance volumes as for mass balance, the internal energy change of the chambers can be denoted as follows:

$$\frac{\mathrm{d}U_1}{\mathrm{d}t} = \sigma_C i_C - \sigma_{PV} i_{PV} - \sigma_{MVin} i_3 + Q_1, \tag{7}$$

$$\frac{\mathrm{d}U_2}{\mathrm{d}t} = \sigma_{PV} i_{PV} - \sigma_S i_2 + Q_2, \tag{8}$$

$$\frac{\mathrm{d}U_3}{\mathrm{d}t} = \sigma_{MVout} i_3 + Q_3. \tag{9}$$

The state equation for chamber gas temperatures can be obtained from the internal energy:

$$\frac{\mathrm{d}U}{\mathrm{d}t} = \frac{\mathrm{d}\left(\mathsf{c}_v m T\right)}{\mathrm{d}t} = \mathsf{c}_v T \frac{\mathrm{d}m}{\mathrm{d}t} + \mathsf{c}_v m \frac{\mathrm{d}T}{\mathrm{d}t}. \tag{10}$$

The derived state equations (considering air flow directions shown in *Fig. 2*) for absolute gas pressures using the ideal gas equation ($pV = m\mathsf{R}T$) are as follows:

$$\begin{aligned}\frac{\mathrm{d}p_1}{\mathrm{d}t} &= \frac{p_1}{m_1}\left(\sigma_C - \sigma_{PV} - \sigma_{MVin}\right) \\ &\quad + \frac{p_1}{T_1}\left(\kappa \frac{\sigma_C T_C - \sigma_{PV} T_1 - \sigma_{MVin} T_1}{m_1} - \frac{k_1 A_1 \left(T_1 - T_{env}\right)}{\mathsf{c}_v m_1}\right. \\ &\quad \left. - \frac{T_1}{m_1}\left(\sigma_C - \sigma_{PV} - \sigma_{MVin}\right)\right),\end{aligned} \tag{11}$$

$$\begin{aligned}\frac{\mathrm{d}p_2}{\mathrm{d}t} &= \frac{p_2}{m_2}\left(\sigma_{PV} - \sigma_S\right) \\ &\quad + \frac{p_2}{T_2}\left(\kappa \frac{\sigma_{PV} T_1 - \sigma_S T_2}{m_2} - \frac{k_2 A_2 \left(T_2 - T_{env}\right)}{\mathsf{c}_v m_2} - \frac{T_2}{m_2}\left(\sigma_{PV} - \sigma_S\right)\right),\end{aligned} \tag{12}$$

$$\frac{\mathrm{d}p_3}{\mathrm{d}t} = \frac{p_3}{m_3}\sigma_{MVout} + \frac{p_3}{T_3}\left(\kappa \frac{\sigma_{MVout} T_1}{m_3} - \frac{k_3 A_3 \left(T_3 - T_{env}\right)}{\mathsf{c}_v m_3} - \frac{T_3}{m_3}\sigma_{MVout}\right), \tag{13}$$

where

$$\kappa = \frac{\mathsf{c}_p}{\mathsf{c}_v}. \tag{14}$$

2.6.3. Dynamic Equations of the Protection Valve Piston

Newton's second law has been used for constructing the dynamic equations of the protection valve piston transformed into first order form as follows:

$$\frac{\mathrm{d}x_{PV}}{\mathrm{d}t} = v_{PV}, \tag{15}$$

and

$$\frac{\mathrm{d}v_{PV}}{\mathrm{d}t} = \frac{F_{PV1} + F_{PV2} - c_{PV}\,(x_{PV} + x_{0PV}) - \mathsf{k}_{PV} v_{PV} - p_3 \frac{d_1^2}{4}\pi + F_{PV\,\mathrm{lim}}}{m_{PV}}, \tag{16}$$

where F_{PV1} and F_{PV2} denote the force generated by input and output chamber pressures, respectively. $F_{PV\,\mathrm{lim}}$ includes the stroke limiting force.

2.6.4. Dynamic Equations of the Magnet Valve Body

Similarly, Newton's second law has been used for the balance of magnet valve body:

$$\frac{\mathrm{d}x_{MV}}{\mathrm{d}t} = v_{MV}, \tag{17}$$

and

$$\frac{\mathrm{d}v_{MV}}{\mathrm{d}t} = \frac{F_{MV} - c_{MV}\,(x_{MV} + x_{0MV}) - \mathsf{k}_{MV} v_{MV} + F_{MV\,\mathrm{lim}}}{m_{MV}}, \tag{18}$$

where F_{MV} and $F_{MV\,\mathrm{lim}}$ denote the magnetic and stroke limiting forces, respectively.

2.6.5. Electromagnetic Dynamic Equations

The relationship between voltage and current is as follows:

$$U = R\,I + L\frac{\mathrm{d}I}{\mathrm{d}t} + I\frac{\mathrm{d}L}{\mathrm{d}t}, \tag{19}$$

where U is the input voltage, R denotes the ohmic resistance. The inductance of the solenoid can be written as:

$$L = \frac{N^2}{R_\Sigma}. \tag{20}$$

In the above equation N is the number of solenoid turns and R_Σ is the valve position-dependent magnetic resistance. In *Eq.* (19), $\frac{\mathrm{d}L}{\mathrm{d}t}$ can be expressed as $\frac{\mathrm{d}L}{\mathrm{d}x_{MV}}\frac{\mathrm{d}x_{MV}}{\mathrm{d}t}$, and $\frac{\mathrm{d}L}{\mathrm{d}x_{MV}}$ can be written as $\frac{\mathrm{d}L}{\mathrm{d}R_\Sigma}\frac{\mathrm{d}R_\Sigma}{\mathrm{d}x_{MV}}$, so the equation can be rewritten in state variable form:

$$\frac{\mathrm{d}I}{\mathrm{d}t} = \frac{U}{L} - \frac{R\,I}{L} - \frac{I}{L}\frac{\mathrm{d}L}{\mathrm{d}R_\Sigma}\frac{\mathrm{d}R_\Sigma}{\mathrm{d}x_{MV}}v_{MV}. \tag{21}$$

2.7. Constitutive Equations

To complete the above equations, some additional algebraic constraints are needed to be defined such as transfer rates, property relations, equipment constraints and defining equations for other characterizing variables.

2.7.1. Force Balance of the Protection Valve Piston

On the upper side, the protection valve piston is affected by a cylindrical spring and the control pressure (p_3). On the lower side it is affected by the pressure distribution in the inner circular section (output side - p_2) and outer ring section (input side - p_1).

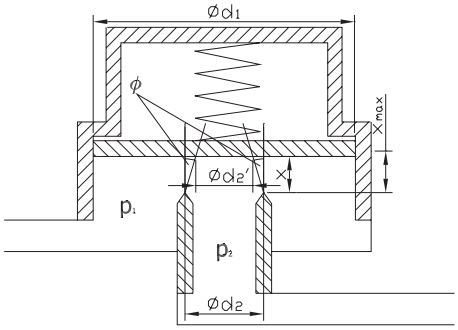

Fig. 4. Model for piston force balance

To evaluate the delimitation between input and output pressures, a grey-box model is used with a governing variable of a cone pitch angle (φ). The cross-section of this cone and the piston determines the border between input and output side pressure surfaces (see *Fig. 4*). The relationship is considered in the following linear form:

$$\varphi = a_1 + a_2 s_{PV}, \tag{22}$$

where s_{PV} is the air speed at the *vena contracta*. The force acting on the donut surface can be written as:

$$F_{PV1} = p_1 \left(\frac{d_1^2}{4} - \frac{(d_2 - 2x\ tg(\varphi))^2}{4} \right) \pi. \tag{23}$$

F_{PV2} is generated on the inner circular surface (determined by d_2):

$$F_{PV2} = p_2 \frac{(d_2 - 2x\ tg(\varphi))^2}{4} \pi. \tag{24}$$

The stroke limiting force of protection valve piston is derived in section 2.5.

2.7.2. Airflow Properties of the Protection Valve

The streaming cross-section of the protection valve can be calculated as:

$$A_{PV} = x_{PV} d_2 \pi. \tag{25}$$

The local gas speed in the protection valve at *vena contracta* is:

$$s_{PV} = \sqrt{2\frac{\kappa}{\kappa-1}\mathrm{R}T_1\left[1-\left(\frac{p_2}{p_1}\right)^{\frac{\kappa-1}{\kappa}}\right]}. \tag{26}$$

The mass flow through the protection valve is written as:

$$\sigma_{PV} = \alpha_{PV} A_{PV} \sqrt{2\frac{\kappa}{\kappa-1}\frac{p_1 m_1}{V_1}\left[\left(\frac{p_2}{p_1}\right)^{\frac{2}{\kappa}}-\left(\frac{p_2}{p_1}\right)^{\frac{\kappa+1}{\kappa}}\right]}. \tag{27}$$

2.7.3. Force Balance of the Magnet Valve Body

Since magnet valve is not excited and has $x_{MV\,\max}$ stroke, the stroke limiting force is:

$$F_{MV\,\lim} = -c_{MV\,\lim}\left(x_{MV} - x_{MV\,\max}\right). \tag{28}$$

The energy conservation balance of the magnetic field determines the minimum field energy. So the force developed by the magnetic field is:

$$F_{MV} = -\frac{\partial E_{MV}}{\partial x_{MV}} = \frac{(N\,I)^2}{2R_\Sigma^2}\frac{\mathrm{d}R_\Sigma}{\mathrm{d}x_{MV}}. \tag{29}$$

The connected magnetic resistances (see *Fig. 5*) are related to the frame (R_{MF}), the plug (R_{MP}), the valve body (R_{MB}), the air clearance between the overlapping coaxial cylindrical surfaces of the valve body and the frame (R_{MC1}) and resistance in the air clearance between the plug and the valve body (R_{MC2}).

The only component that depends on the stroke is R_{MC2}, which is proportional to x_{MV}. R_{MF}, R_{MP}, and R_{MC2} remain unchanged during valve body displacement. The change of R_{MB} is negligibly small, so it is considered constant as well.

The magnetic resistance can be calculated as function of the magnet valve body stroke from the magnetic circuit shown in *Fig. 5*:

$$R_\Sigma = R_{MP} + R_{MF} + R_{MC1} + R_{MC2} + R_{MB}. \tag{30}$$

Since there is only one stroke-dependent component, the derivative function with respect to x_{MV} is written as:

$$\frac{dR_\Sigma}{dx_{MV}} = \frac{dR_{MC2}}{dx_{MV}} = \frac{1}{\mu_0 A_{MB}}. \tag{31}$$

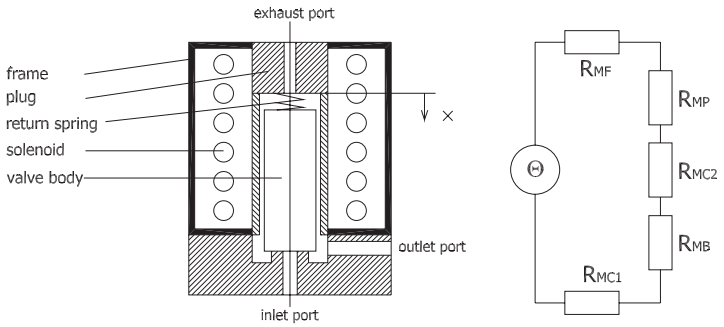

Fig. 5. Scheme of the solenoid valve and its magnetic model

2.7.4. Airflow Properties of the Magnet Valve

The magnet valve exhaust cross-section can be calculated as:

$$A_{MVexh} = \frac{d_{MVexh}^2 \pi}{4}. \tag{32}$$

The inlet port cross-section is as follows:

$$A_{MVin} = (x_{MV\max} - x_{MV})\, d_{MVin} \pi. \tag{33}$$

According to the magnet valve streaming cross-section assumption ($\mathcal{A}8$), the control chamber pressure can be used as internal pressure level inside the magnet valve. This means that the inlet and exhaust air flows are defined by pressure rate between the control chamber pressure and the corresponding port pressures. Furthermore, outlet airflow is determined by the following algebraic equation:

$$\sigma_{MVout} = \sigma_{MVin} - \sigma_{MVexh}. \tag{34}$$

Then the exhaust airflow of the magnet valve is written as:

$$\sigma_{MVexh} = \alpha_{MV} A_{MVexh} \sqrt{2 \frac{\kappa}{\kappa - 1} \frac{p_3 m_3}{V_3} \left[\left(\frac{p_{env}}{p_3} \right)^{\frac{2}{\kappa}} - \left(\frac{p_{env}}{p_3} \right)^{\frac{\kappa+1}{\kappa}} \right]}, \tag{35}$$

and inlet air flow of the magnet valve is:

$$\sigma_{MVin} = \alpha_{MV} A_{MVin} \sqrt{2 \frac{\kappa}{\kappa - 1} \frac{p_1 m_1}{V_1} \left[\left(\frac{p_3}{p_1} \right)^{\frac{2}{\kappa}} - \left(\frac{p_3}{p_1} \right)^{\frac{\kappa+1}{\kappa}} \right]}. \tag{36}$$

3. Nonlinear State Space Representation

The above developed model of the protection valve is obtained in the form of a set of differential-algebraic equations (DAEs). This section is devoted to the derivation of a lumped nonlinear state space model in its standard input-affine form from this engineering model.

3.1. System Variables

The important system variables are described here that are used in the nonlinear state space model of the valve such as the state vector, disturbance vector, input and outputs.

3.1.1. State Vector of the Nonlinear Model

From the conservation *Eqs.* (4), (5), (6), (11), (12), (13), (15), (16), (17), (18) and (21) the state vector is formed from their differential variables as:

$$\underline{q} = \begin{bmatrix} m_1 & p_1 & m_2 & p_2 & m_3 & p_3 & x_{PV} & v_{PV} & x_{MV} & v_{MV} & I \end{bmatrix}^T . \tag{37}$$

3.1.2. Disturbance Vector

The uncontrollable inputs are formed as disturbance vector as follows:

$$\underline{d} = \begin{bmatrix} \sigma_C & T_C & \sigma_S & T_S & T_{env} & p_{env} \end{bmatrix}^T . \tag{38}$$

3.1.3. Input Vector

The control input vector includes one member only, which is the excitation voltage of the magnet valve:

$$\underline{u} = [U] . \tag{39}$$

3.1.4. Outputs

The measured output includes the input and output chamber pressures, respectively:

$$\underline{y} = \begin{bmatrix} p_1 & p_2 & p_3 & I \end{bmatrix}^T . \tag{40}$$

The performance output is the output chamber pressure:

$$\underline{z} = [p_2] . \tag{41}$$

3.2. State Equations

Substituting the constitutive equations into the differential conservation balances the following state space model is obtained in input-affine form where the input matrix $\underline{B}$ is linear:

$$\frac{d\underline{q}(t)}{dt} = f(\underline{q}(t), \underline{d}(t)) + \underline{B}(\underline{q}(t))\underline{u}(t). \tag{42}$$

The above state equation can be expanded as:

$$\begin{bmatrix} \dot{m}_1 \\ \dot{p}_1 \\ \dot{m}_2 \\ \dot{p}_2 \\ \dot{m}_3 \\ \dot{p}_3 \\ \dot{x}_{PV} \\ \dot{v}_{PV} \\ \dot{x}_{MV} \\ \dot{v}_{MV} \\ \dot{I} \end{bmatrix} = \begin{bmatrix} f_1(\underline{q}(t), \underline{d}(t)) \\ f_2(\underline{q}(t), \underline{d}(t)) \\ f_3(\underline{q}(t), \underline{d}(t)) \\ f_4(\underline{q}(t), \underline{d}(t)) \\ f_5(\underline{q}(t), \underline{d}(t)) \\ f_6(\underline{q}(t), \underline{d}(t)) \\ f_7(\underline{q}(t), \underline{d}(t)) \\ f_8(\underline{q}(t), \underline{d}(t)) \\ f_9(\underline{q}(t), \underline{d}(t)) \\ f_{10}(\underline{q}(t), \underline{d}(t)) \\ f_{11}(\underline{q}(t), \underline{d}(t)) \end{bmatrix} + \begin{bmatrix} 0 \\ 0 \\ 0 \\ 0 \\ 0 \\ 0 \\ 0 \\ 0 \\ 0 \\ 0 \\ \frac{(R_{MF}+R_{MP}+\frac{x_{MV}}{\mu_0 A_{MB}}+R_{MC1}+R_{MB})}{N^2} \end{bmatrix} u(t), \tag{43}$$

where the nonlinear state functions with all constitutive relations substituted are:

$$f_1(\underline{q}(t), \underline{d}(t)) = \sigma_C - \alpha_{PV} d_2 \pi x_{PV} \sqrt{\frac{2\kappa p_1 m_1 \left((\frac{p_2}{p_1})^{\frac{2}{\kappa}} - (\frac{p_2}{p_1})^{\frac{\kappa+1}{\kappa}} \right)}{(\kappa-1)V_1}} - \\ - \alpha_{MV} d_{MVin} \pi x_{MV} \sqrt{\frac{2\kappa p_1 m_1 \left((\frac{p_3}{p_1})^{\frac{2}{\kappa}} - (\frac{p_3}{p_1})^{\frac{\kappa+1}{\kappa}} \right)}{(\kappa-1)V_1}}, \tag{44}$$

$$f_2(\underline{q}(t), \underline{d}(t)) = \frac{\kappa \sigma_C T_c m_1 \mathsf{R} - \kappa \alpha_{PV} d_2 \pi x_{PV} \sqrt{\frac{2\kappa p_1 m_1 \left((\frac{p_2}{p_1})^{\frac{2}{\kappa}} - (\frac{p_2}{p_1})^{\frac{\kappa+1}{\kappa}} \right)}{(\kappa-1)V_1}} p_1 V_1}{m_1 V_1} + \\ + \frac{k_1 A_1 T_{env} m_1 \mathsf{R} - \kappa \mathsf{c}_v \alpha_{MV} d_{MV} \pi x_{MV} \sqrt{\frac{2\kappa p_1 m_1 \left((\frac{p_3}{p_1})^{\frac{2}{\kappa}} - (\frac{p_3}{p_1})^{\frac{\kappa+1}{\kappa}} \right)}{(\kappa-1)V1}} p_1 V_1 - k_1 A_1 p_1 V_1}{m_1 V_1 \mathsf{c}_v}, \tag{45}$$

$$f_3(\underline{q}(t),\underline{d}(t)) = \alpha_{PV} d_2 \pi x_{PV} \sqrt{\frac{2\kappa p_1 m_1 \left((\frac{p_2}{p_1})^{\frac{2}{\kappa}} - (\frac{p_2}{p_1})^{\frac{\kappa+1}{\kappa}} \right)}{(\kappa-1)V_1}} - \sigma_S, \tag{46}$$

$$f_4(\underline{q}(t),\underline{d}(t)) = \frac{\kappa \alpha_{PV} d_2 \pi x_{PV} \sqrt{\frac{2\kappa p_1 m_1 \left((\frac{p_2}{p_1})^{\frac{2}{\kappa}} - (\frac{p_2}{p_1})^{\frac{\kappa+1}{\kappa}} \right)}{(\kappa-1)V_1}} p_1 V_1}{V_2 m_1} + \\ + \frac{k_2 A_2 T_{env} m_2 \mathsf{R} - \kappa \mathsf{c}_v \sigma_S p_2 V_2 - k_2 A_2 p_2 V_2}{m_2 V_2 \mathsf{c}_v}, \tag{47}$$

$$f_5(\underline{q}(t),\underline{d}(t)) = \alpha_{MV} d_{MVin} \pi x_{MV} \sqrt{\frac{2\kappa p_1 m_1 \left((\frac{p_3}{p_1})^{\frac{2}{\kappa}} - (\frac{p_3}{p_1})^{\frac{\kappa+1}{\kappa}} \right)}{(\kappa-1)V_1}}, \tag{48}$$

$$f_6(\underline{q}(t),\underline{d}(t)) = \\ = \frac{\kappa \alpha_{MV} d_{MV} \pi x_{MV} \sqrt{\frac{2\kappa p_1 m_1 \left((\frac{p_3}{p_1})^{\frac{2}{\kappa}} - (\frac{p_3}{p_1})^{\frac{\kappa+1}{\kappa}} \right)}{(\kappa-1)V_1}} p_1 V_1 m_3 \mathsf{c}_v - k_3 A_3 m_1 p_3 V_3 + k_3 A_3 m_1 T_{env} m_3 \mathsf{R}}{m_3 V_3 m_1 \mathsf{c}_v}, \tag{49}$$

$$f_7(\underline{q}(t),\underline{d}(t)) = v_{PV}, \tag{50}$$

$$f_8(\underline{q}(t),\underline{d}(t)) = \\ = \frac{p_1 (\frac{d_1^2}{4} - \frac{d_2^2}{4})\pi + \frac{1}{4} p_2 \pi d_2^2 - \mathsf{c}_{PV}(x_{PV} + x_{0PV}) - \mathsf{k}_{PV} v_{PV} - \frac{1}{4} p_{env} d_1^2 \pi}{m_{PV}}, \tag{51}$$

$$f_9(\underline{q}(t),\underline{d}(t)) = v_{MV}, \tag{52}$$

$$f_{10}(\underline{q}(t),\underline{d}(t)) = \\ = \frac{\frac{N^2 I^2}{2(R_{MF}+R_{MP}+\frac{x_{MV}}{\mu_0 A_{MB}}+R_{MC1}+R_{MB})^2 \mu_0 A_{MB}} - c_{MV}(x_{MV} + x_{0MV}) - \mathsf{k}_{MV} v_{MV}}{m_{MV}}, \tag{53}$$

$$f_{11}(\underline{q}(t),\underline{d}(t)) = \frac{I v_{MV}}{(R_{MF} + R_{MP} + \frac{x_{MV}}{\mu_0 A_{MB}} + R_{MC1} + R_{MB})\mu_0 A_{MB}} - \\ - \frac{RI(R_{MF} + R_{MP} + \frac{x_{MV}}{\mu_0 A_{MB}} + R_{MC1} + R_{MB})}{N^2}. \tag{54}$$

3.3. Output Equations

Since the output is linear with respect to the state vector, the output equation can be simplified as:

$$\underline{y} = \underline{C}\underline{q}(t), \tag{55}$$

where the output matrix is:

$$\underline{C} = \begin{bmatrix} 0 & 1 & 0 & 0 & 0 & 0 & 0 & 0 & 0 & 0 & 0 \\ 0 & 0 & 0 & 1 & 0 & 0 & 0 & 0 & 0 & 0 & 0 \\ 0 & 0 & 0 & 0 & 0 & 1 & 0 & 0 & 0 & 0 & 0 \\ 0 & 0 & 0 & 0 & 0 & 0 & 0 & 0 & 0 & 0 & 1 \end{bmatrix}. \tag{56}$$

The performance output is then created using the measured output as follows:

$$\underline{z} = \underline{L}\underline{y} = \begin{bmatrix} 0 & 1 & 0 & 0 \end{bmatrix} \begin{bmatrix} p_1 \\ p_2 \\ p_3 \\ I \end{bmatrix}. \tag{57}$$

4. Model Verification

The verification of the developed non-linear model is performed by extensive simulation experiments using MATLAB/SIMULINK model against engineering intuition and operation experience on the quantitative behavior of the system.

To obtain the model solutions the stiff ODE23s solver (Modified Rosenbrock formula [10]) with variable step size has been used. The solver setup included relative tolerance requirement of 10^{-8}. Parameters considered in simulation calculations can be seen in *Table 1* in the Appendix.

4.1. Simulation Results

The simulation calculations considered three typical operating situations. Two of them are executed without modulation of the magnet valve. The third is investigated with magnet valve excitation in order to see the effect of active magnet valve on the output chamber pressure.

4.1.1. System Fill Up Process

This case is simulated with constant compressor fill airflow and constant filling gas temperature (accomplished by intercooling). The initial state vector is as follows:

$$\underline{q}^* = \begin{bmatrix} 0.844 & 7.1 \cdot 10^5 & 1.19 \cdot 10^{-3} & 10^5 & 5.94 \cdot 10^{-6} & 10^5 & 0 & 0 & 7 \cdot 10^{-4} & 0 & 0 \end{bmatrix}^T. \tag{58}$$

The disturbance vector is considered as:

$$\underline{d}^* = \begin{bmatrix} 10^{-2} & 293 & 0 & 293 & 293 & 10^5 \end{bmatrix}^T . \tag{59}$$

The dynamic response functions are shown in the Appendix (See *Fig. 6*). The responses agree with the engineering expectations: in fill up case the input chamber pressure increased, after reaching the dynamic opening pressure of the protection valve the valve stroke increases and, as a consequence, the output chamber pressure increases as well.

4.1.2. Circuit Defect Situation

This case was simulated with constant diameter leakage of circuit to the 10^5 Pa environment pressure starting from the common $7 \cdot 10^6$ Pa pressure level. No input side airflow was considered. The initial state vector is as follows:

$$\underline{q}^* = \begin{bmatrix} 0.833 & 7 \cdot 10^5 & 8.33 \cdot 10^{-3} & 7 \cdot 10^5 & 5.94 \cdot 10^{-6} & 10^5 & 2.5 \cdot 10^{-3} & 0 & 7 \cdot 10^{-4} & 0 & 0 \end{bmatrix}^T . \tag{60}$$

The initial disturbance vector is considered as:

$$\underline{d}^* = \begin{bmatrix} 0 & 293 & 0 & 293 & 293 & 10^5 \end{bmatrix}^T . \tag{61}$$

In this case, the brake system consumption term (σ_S) in the disturbance vector is function of output chamber gas mass and pressure as follows:

$$\sigma_S = \alpha_S A_S \sqrt{\frac{2\kappa}{\kappa - 1} \frac{p_2 m_2}{V_2} \left[\left(\frac{p_{env}}{p_2} \right)^{\frac{2}{\kappa}} - \left(\frac{p_{env}}{p_2} \right)^{\frac{\kappa+1}{\kappa}} \right]}, \tag{62}$$

where the contraction coefficient (α_S) is considered 0.8 and streaming cross-section (A_S) as a 8 mm diameter hole.

The dynamic response functions are shown in the Appendix (see *Fig. 7*). In circuit defect case input and output chamber pressures decreased as expected. On reaching the dynamic closing pressure of the protection valve, the valve stroke decreases and finally it closes, so the input chamber is protected against the damaged circuit.

4.1.3. Circuit Pressure Limiting

This case is investigated with zero compressor charge. The high pressure input chamber fills the circuit that is pressure limited when the magnet valve becomes

activated. The magnet valve is activated for constant 38 ms intervals after 45 ms deactivation time. The initial state vector is as follows:

$$\underline{q}^* = \left[\, 1.545 \;\; 1.3 \cdot 10^6 \;\; 8.32 \cdot 10^{-3} \;\; 7 \cdot 10^5 \;\; 7.72 \cdot 10^{-5} \;\; 1.3 \cdot 10^6 \;\; 0 \;\; 0 \;\; 0 \;\; 0 \;\; 0.8 \,\right]^T . \tag{63}$$

The initial disturbance vector is considered as:

$$\underline{d}^* = \left[\, 0 \quad 293 \quad 0 \quad 293 \quad 293 \quad 10^5 \,\right]^T . \tag{64}$$

The dynamic response functions are shown in the Appendix (see *Fig.8*). As seen in the figures, after a certain retardation time the magnet valve releases and exhausts the control chamber. Through that the protection valve opens and fills the circuit. After a new solenoid excitation the control chamber is filled up again and the protection valve is closed by that. This is a realization of the circuit pressure limiting base cycle.

5. Conclusions

A nonlinear hybrid model of a single protection valve with extension of a magnetic valve has been developed from first engineering principles using fluid-, thermo-, magneto-dynamic and mechanical considerations. The model is obtained in a DAE form where the constitutive equations can be substituted into the dynamic conservation balance equations.

A lumped nonlinear input-affine state space model has been developed from the above dynamic engineering model where the disturbance, control input and output variables together with the state variables and model parameters have also been identified. The input function of the input-affine nonlinear state space model has been found to be a simple linear function of the states.

The developed model is able to predict the dynamic behavior of the real system with the accuracy needed for controller design purposes. The model has been analyzed from computational point of view and has been verified in three cases against engineering intuition by simulation studies.

Acknowledgements

The authors are indebted to Dr. Tamás Gausz, Associate Professor of Department of Aircraft and Ships at Budapest University of Technology and Economics, and Ansgar Fries, Head of Knorr-Bremse R&D Budapest for their useful advice in preparation of the presented model.

Part of this work has been supported by the Hungarian National Research Fund through grant T032479 which is gratefully acknowledged.

References

[1] NÉMETH, H. – AILER, P. – HANGOS, K. M., Nonlinear Hybrid Model of Single Protection Valve for Pneumatic Brake Systems, *Research Report of Computer and Automation Research Institute*, Budapest, Hungary, SCL-002/2002, 2002.

[2] NÉMETH, H. – PALKOVICS, L. – BOKOR, J., Electro-Pneumatic Protection Valve with Robust Control for Commercial Vehicle Air Supply Systems, *Proc. of 6th International Symposium on Advanced Vehicle Control '02*, Hiroshima, Japan, 2002, pp. 757–762.

[3] AILER, P. – SÁNTA, I. – SZEDERKÉNYI, G. – HANGOS, K. M., Nonlinear Model-Building of a Low-Power Gas Turbine, *Periodica Polytechnica Ser. Transportation Eng.*, **29** No. 1-2 (2001), pp. 117–135.

[4] AILER, P. – SZEDERKÉNYI, G. – HANGOS, K. M., Modelling and Nonlinear Analysis of a Low-Power Gas Turbine, *Research Report of Computer and Automation Research Institute*, Budapest, Hungary, SCL-001/2001, 2001.

[5] HANGOS, K. M. – CAMERON, I., Process Modelling and Model Analysis. *Process Systems Engineering*, **4**, Academic Press, London, 2001.

[6] LJUNG, L. – GLAD, T., *Modeling of Dynamic Systems*, Prentice Hall, Englewood Cliffs, N.J., 1994.

[7] SZENTE, V. – VAD, J. – LÓRÁNT, G. – FRIES, A., Computational and Experimental Investigation on Dynamics of Electric Braking Systems, *Proc. 7th Scandinavian International Conference on Fluid Power*, May 2001, Linköping, Sweden, **I** (2001), pp. 263–275.

[8] SZENTE, V. – VAD, J., Computational and Experimental Investigation on Solenoid Valve Dynamics, *Proc. 2001 IEEE/ASME International Conference on Advanced Intelligent Mechatronics*, July 2001, Como, Italy, **I** (2001), pp. 618–623.

[9] ISTÓK, B. – VAD, J. – SZABÓ, ZS. – GÁSPÁR, T. – NÉMETH, H. – LÓRÁNT, G., On the Resonance Effects of Pneumatic Unloader Valves, *3rd International Fluid Power Conference*, Aachen, Germany, **2** (2002), pp. 581–592.

[10] SHAMPINE, L. F. – REICHELT, M. W., The MATLAB ODE Suite, *SIAM Journal on Scientific Computing*, **18** (1997), pp. 1–22.

A. Appendix – Nomenclature

Variables

a	pressure distribution factor [-;s/m]
A	area, surface [m^2]
α	contraction coefficient [-]
c	spring coefficient [N/m]
c	specific heat [J/kgK]
d	diameter [m]
F	force [N]
φ	angle [-]
i	enthalpy [J/kgK]
I	electric current [A]
k	heat transmission coefficient [W/m^2K]
k	damping coefficient [Ns/m]
κ	adiabatic exponent [-]
L	inductance [Vs/A]
m	mass [kg]
σ	air flow [kg/s]
μ	permeability [Vs/Am]
N	solenoid turns [-]
p	absolute pressure [Pa]
Q	heat energy flow [W/kgK]
R	resistance [electric-Ω; magnetic-A/Vs]
R	specific gas constant [J/kgK]
s	gas speed [m/s]
t	time [s]
T	absolute temperature [K]
U	voltage [V]
v	speed [m/s]
V	volume [m^3]
x	stroke [m]

Indices

$_0$	refers to initial state or vacuum
$_1$	refers to input chamber
$_2$	refers to output chamber
$_3$	refers to control chamber
$_{PV}$	refers to protection valve
$_{MV}$	refers to magnet valve
$_C$	refers to compressor
$_S$	refers to brake system

env	refers to environment
v	refers to constant volume
p	refers to constant pressure
in	refers to inlet
out	refers to outlet
exh	refers to exhaust
max	refers to maximum
lim	refers to limitation
Σ	refers to magnetic resultant
MP	refers to magnet valve plug part
MF	refers to magnet valve frame
MJ	refers to magnet valve jacket
MB	refers to magnet valve body
$MC1$	refers to magnet valve air clearance 1
$MC2$	refers to magnet valve air clearance 2

B. Appendix – Figures of Simulations

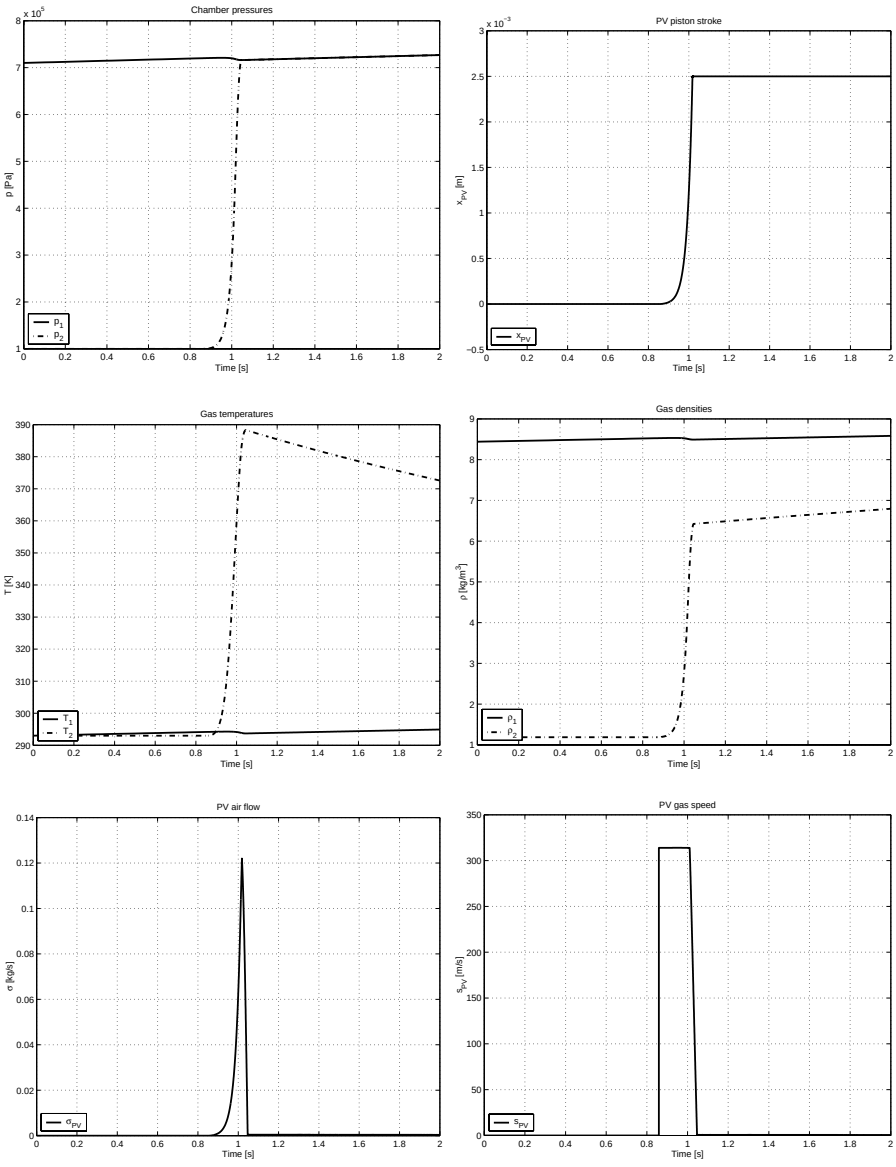

Fig. 6. Circuit fill up process

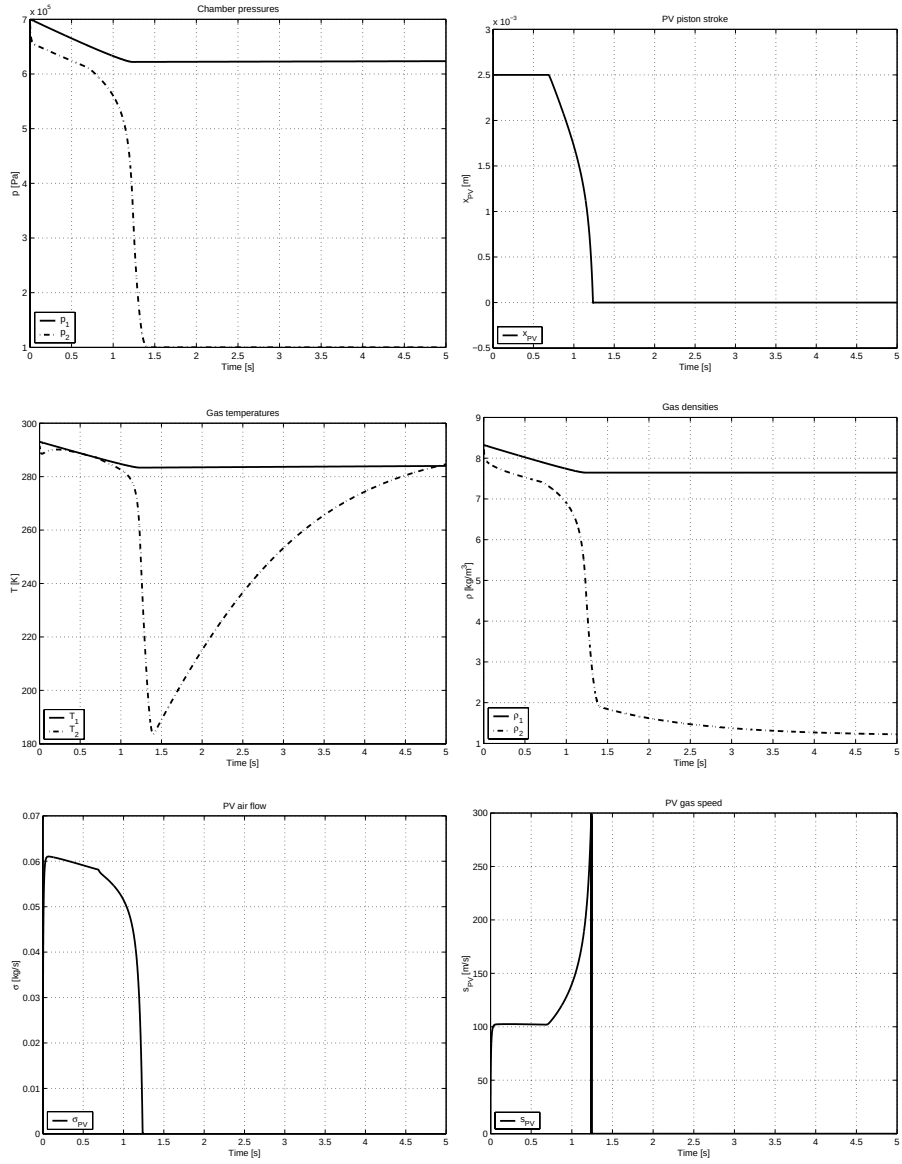

Fig. 7. Circuit defect situation

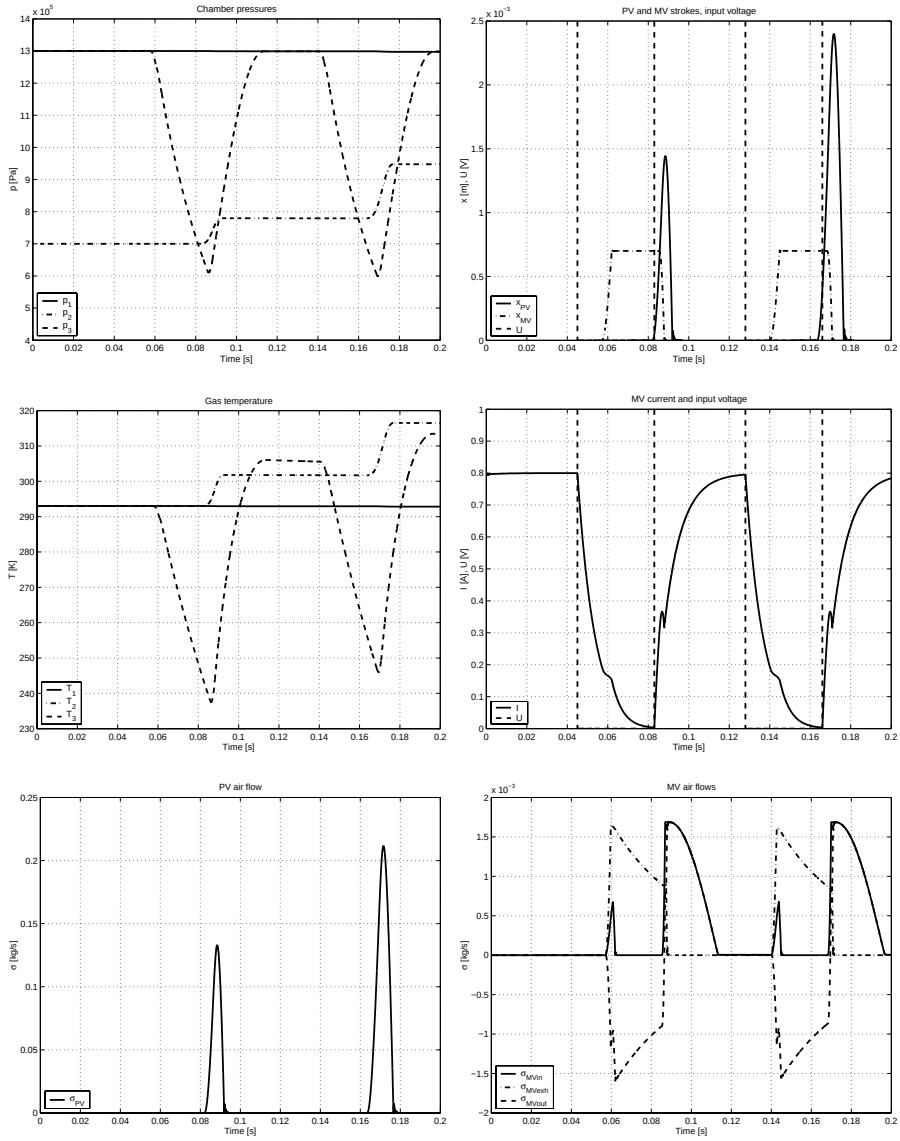

Fig. 8. Circuit pressure limiting with magnet valve

C. Appendix – Model Parameters

Table 1. Model parameters used for the simulation

Parameter name	Symbol	Unit	Value
Pressure distribution parameter1 of protection valve	a_1	rad	0
Pressure distribution parameter2 of protection valve	a_2	rad s/m	0.0002
Input chamber surface area	A_1	m^2	0.1
Output chamber surface area	A_2	m^2	0.01
Control chamber surface area	A_3	m^2	0.001
Magnet valve contraction coefficient	α_{MV}	–	0.7
Contraction coefficient	α_{PV}	–	0.8
Stiffness of spring	c_{MV}	N/m	1100
Stiffness of stroke limiter of magnet valve	c_{MVlim}	N/m	10^7
Stiffness of spring	c_{PV}	N/m	15000
Stiffness of stroke limiter of protection valve	c_{PVlim}	N/m	$2.8 \cdot 10^8$
Diameter of protection valve piston	d_1	m	0.023
Valve seat diameter of protection valve	d_2	m	0.012
Magnet valve body diameter	d_{MB}	m	0.008
Magnet valve inlet diameter	d_{MVin}	m	0.001
Magnet valve exhaust diameter	d_{MVexh}	m	0.001
Input chamber heat transfer coefficient	k_1	W/m^2K	100
Output chamber heat transfer coefficient	k_2	W/m^2K	100
Control chamber heat transfer coefficient	k_3	W/m^2K	100
Damping coefficient of magnet valve	k_{MV}	Ns/m	10
Damping coefficient of protection valve	k_{PV}	Ns/m	50
Adiabatic exponent	κ	–	1.4
Mass of magnet valve body	m_{MV}	kg	0.002
Mass of protection valve piston	m_{PV}	kg	0.02
Permeability of vacuum	μ_0	Vs/Am	$4\pi \cdot 10^7$
Number of solenoid turns	N	–	2200
Electric resistance of magnet valve	R	Ω	30
Magnetic resistance of valve body	R_{MB}	A/Vs	10^4
Magnetic resistance of air clearance1	R_{MC1}	A/Vs	$1.9 \cdot 10^7$
Magnetic resistance of magnet valve frame	R_{MF}	A/Vs	10^4
Magnetic resistance of plug part	R_{MP}	A/Vs	10^4
Specific gas constant	R	J/kgK	287.14
Input chamber volume	V_1	m^3	0.1
Output chamber volume	V_2	m^3	0.001
Control chamber volume	V_3	m^3	0.000005
Spring preset stroke of magnet valve	x_{MV0}	m	0.0025
Maximal magnet valve stroke	x_{MVmax}	m	0.0007
Spring preset yield stroke	x_{PV0}	m	0.0125
Maximal piston stroke	x_{PVmax}	m	0.0025